Eur. Phys. J. D **43**, 295–298 (2007)
DOI: 10.1140/epjd/e2007-00101-2

THE EUROPEAN PHYSICAL JOURNAL D

Structure and electrical conduction of WO_3 nanorods epitaxially grown on mica

M. Gillet[1,a], R. Delamare[1], and E. Gillet[2]

[1] Université Paul Cézanne–Aix Marseille III, Faculté des sciences et techniques, Case 151, 52 avenue Escadrille Normandie Niemen, 13397 Marseille Cedex 20, France
[2] Department of Electronics and Vacuum Physics, Faculty of Mathematics and Physics Charles University, V. Holesovickach 2, 180000 Prague, Czech Republic

Received 25 July 2006 / Received in final form 2nd November 2006
Published online 24 May 2007 –

Abstract. Tunsten oxide nanorods are grown on mica substrate in air from WO_3 vapor at 590 °C. They are epitaxially oriented on the substrate in three directions according to the hexagonal symmetry of the mica. Their morphology was investigated by Atomic Force Microscopy (AFM), their structure by Electron Diffraction (ED) and High Resolution Electron Microscopy (HRTEM). The energy dispersive X-ray analysis (EDX) associated with the TEM revealed the presence of potassium in the first step of the nanostructures growth suggesting the formation of a tungsten bronze. According to their thickness the nanorods have a structure either hexagonal or monoclinic. The structural investigations showed that numerous kinds of planar defects parallel to the growth direction are formed. The electrical conduction was analyzed with a Conductive Atomic Force Microscopy (CAFM) method which allows to obtain either an image of the resistance variations along the nanorods or a current-voltage response. The result demonstrates that the WO_3 nanorods form electrically networks suitable for gas sensing experiments.

PACS. 81.10.-h Methods of crystal growth; physics of crystal growth – 61.46.-w Nanoscale materials – 73.63.-b Electronic transport in nanoscale materials and structures

1 Introduction

Semi conducting metal oxides such as WO_3 have attracted attention as candidates for chemical sensors. This interest is due to the fact that their electrical conductivity depends on the nature and concentration of adsorbed species on their surface. In the recent past years polycrystalline WO_3 thin films have been extensively tested for the sensing properties towards various gases [1–3] and the results evidenced the role of the grain size. The sensing response increases steeply with a decrease of the grain size [4]. However in such polycrystalline thin films the average grain size is difficult to be controlled and may be modified during the sensing process due to the fact that sensors with conventional thin films operate at temperatures ranging between 200 and 500 °C. Recently monocrystalline nanostructures including nanorods and nanobelts of semi conducting oxides have been synthesized [5–14]. Some of the nanostructures have been tested as sensing material for chemical sensors. Due to their large surface to volume ratio and their small dimensions compared to the Debye length, they appear as promising candidates for chemical sensors working at low temperature and even at room temperature. In this paper, we report on the synthesis of tungsten oxide nanorods obtained by a very simple method, on their structure and on their electrical characterization.

[a] e-mail: marcel.gillet@l2mp.fr

2 Nanorods synthesis

The experimental set up used to synthesize the nanorods was described elsewhere [15]. The nanorods are grown on a mica substrate, from WO_3, vapor provided by a tungsten oxide film predeposited on a SiO_2 wafer. The vapour source is heated at a temperature $T_S \cong 600$ °C the mica substrate is located above the source at a distance d and heated by irradiation from the WO_3 source. The temperature mica substrate is determined by the distance d and varies in a range of 450–550 °C. After cooling at a room temperature, the mica substrate exhibits nanorods as presented in Figure 1 which is a typical image obtained with $T_S = 590$ °C and a deposition time of $T_d = 40$ mn. The morphology of the nanorods has been investigated by Atomic Force Microscopy (AFM), their composition by energy dispersive X-Ray spectroscopy (EDX) and their structure was analyzed by High Resolution Electron Microscopy (HRTEM) and Transmission Electron Diffraction (TED). The electrical conduction was characterized by Conductive Atomic Force Microscopy (CAFM).

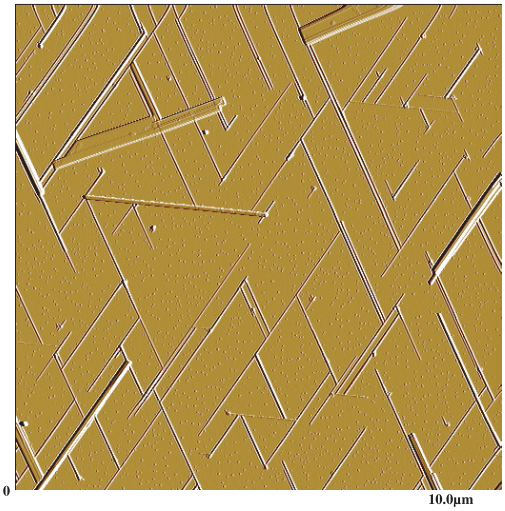

Fig. 1. AFM image of WO_3 nanorods grown on mica. Deposition time: 45 min.

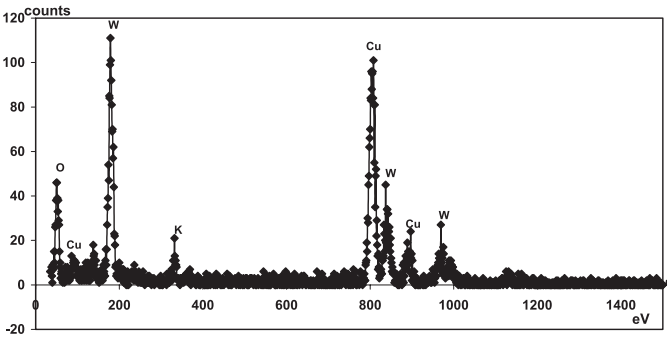

Fig. 2. EDX spectrum of a WO_3 nanorod.

3 Morphology of WO_3 nanorods

The nanorods are grown on a mica substrate. AFM observations show that they are highly aligned, parallel to three directions according to the hexagonal symmetry of the (0001) mica surface proving that they are epitaxially grown. In fact two directions are predominant as it is shown in Figure 1. For given vapour source temperature T_S and the distance d, the WO_3 nanorod size depends on the deposition time T_d. For 30 mn $< T_d <$ 90 mn the nanorod dimensions vary in range 1–20 μm, 10–200 nm and 1–50 nm for the length, width and thickness respectively. The AFM images reveal a variety of features and shapes. Some of them are perfect with constant thickness, however often they are multiple or with incomplete surface layers [15].

4 Composition and structure

Figure 2 represents an EDX spectrum obtained on a nanorod extracted from its mica substrate by means of a transfer replica. The EDX spectrum exhibits peaks which are assigned to Cu coming from the electron microscope grid and peaks assigned to elements W, O and K coming from the nanorods. The relative proportion of K atoms in the nanorods appears to be dependent of the nanorod thickness as indicated by the ratio I_K/I_W of the intensity peaks of K and W which decreases as the thickness increases; for example $I_K/I_W = 0.25$ and 0.11 for nanorods with a thickness of $e = 3.5$ nm and 6 nm respectively. The ED and HRTEM investigations of nanorods show a variety of structures with numerous and complex atomic and planar defects.

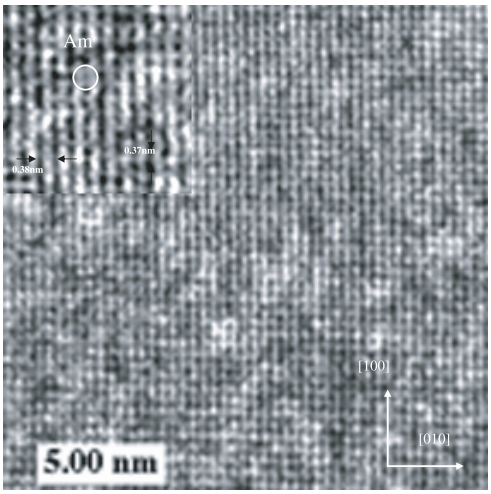

Fig. 3. HRTEM image of a WO_3 nanorod (thickness: 5.5 nm).

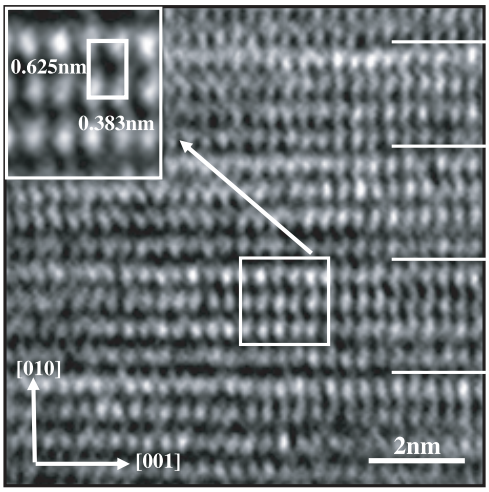

Fig. 4. HRTEM image of a thin nanorod (thickness: 3 nm).

Figure 3 represents an HRTEM image typical of the most nanorods with a thickness larger than 5 nm. It images the atomic structure of the top of the nanorod as a (001) plane with atomic distances $D_1 = 0.37$ nm and $D_2 = 0.38$ nm which are in good agreement with the value of interatomic distances deduced from the electron diffraction pattern. These results are interpreted on the base of a monoclinic tungsten oxide structure. The HRTEM image reveals a quasi perfect crystalline structure with some atomic defects, as it can be seen in A on the enlarged part of the image.

Figure 4 displays an HRTEM image of another nanorod with a thickness of about 3 nm. It exhibits a

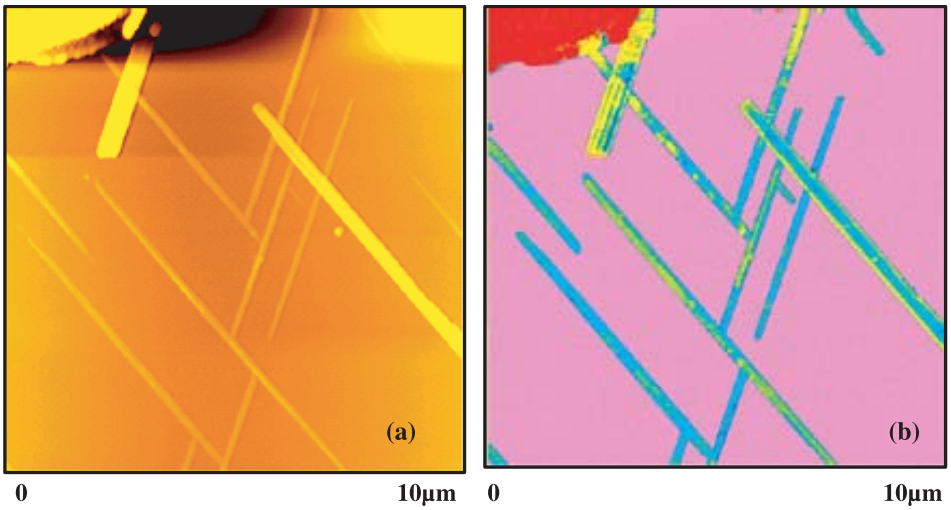

Fig. 5. (Color online) (a) AFM image of a WO_3 nanorod. (b) CAFM image corresponding to (a). The gold electrode is visible on the left upper side of the image.

rectangular basic mesh with dimensions of 0.625 nm and 0.388 nm corresponding to the atomic position of tungsten atoms in the (100) plane of either the hexagonal tungsten oxide (HWO_3) or to the hexagonal tungsten bronze (HTB). The hexagonal tungsten oxide (HWO_3) and the hexagonal tungsten bronze (HTB) crystallize in the same hexagonal structure and with lattices parameters very closed each others [16]. So it is not possible to distinguish between the HWO_3 and the HTB phases on the basis of the electron diffraction patterns and TEM images. However the EDX spectrum indicates the presence of potassium atoms in such nanorods. So we consider that the nanorod consists in an HTB phase on which the HWO_3 grows. The electron diffraction patterns and the HRTEM observations revealed a large variety of planar defects and structural distortions. In the electron diffraction patterns the presence of weak spots between the main spots indicates the existence of ordered planar defects as shown in Figure 4 where superlattice figures running parallel to the [001] direction are shown. In addition, on the electon diffraction pattern of Figure 4 diffuse streaks along the [010] direction indicates that there is numerous disordered plane defects running parallel to the length axis of the nanorod.

From the ED and the HRTEM results we deduce that WO_3 nanorods exhibit either a monoclinic or an hexagonal structure. The monoclinic structure of WO_3 nanorods have a (001) plane parallel to the top surface. The hexagonal WO_3 nanorods have a surface plane parallel to (100) and their length direction parallel to [100] direction. In the two structures the defects planes are parallel to the length direction.

5 Electrical characterization of the WO_3 nanorods

The set up for electrical conduction measurement has been described elsewhere [17]: a gold electrode is deposited on an extremity of the nanorod. The CAFM method allows to measure the electrical current which flows through the nanorod between the gold electrode and the conductive AFM tip. It is possible to obtain simultaneously a topographic image and an image of the resistance (Figs. 5a and 5b). Systematical measurements on many nanorods, evidence that nanorods form networks electrically well connected with relatively small variation of the resistance along the nanorods. From resistance values, we have deduced WO_3 nanorod resistivity which ranges between 10^{-2} and 10^{-3} Ω m. At our knowledge, no resistivity values for monocrystalline WO_3 are available in the literature. The WO_3 resistivity studies concern polycristalline sample and give values of one or more order of magnitude higher [18].

6 Conclusion

It is possible to synthesize tungsten nanorods in a very simple way. The nanorods contain potassium atoms coming from the mica substrate. The Electron Diffraction and High Resolution Transmission Electron Microscopy studies show that WO_3 nanorods have two crystallines structures according to their size: thin nanorods exhibit a hexagonal structure while thicker ones have a monoclinic structure. These results suggest that the first step of growth involves the formation of a very thin potassium compound with an hexagonal structure, epitaxially oriented on the mica substrate. We suppose that this compound is an hexagonal tunsten bronze. Further growth proceeds by the deposition of the monoclinic tunsten oxide which matches the hexagonal tungsten bronze.The CAFM investigations demonstrate that the nanorods form a network of electrically connected 1-D nanostructure which can be tested as sensing device.

This work is supported by the E.C. Contract STRP- 505895 – NanoChemSens.

References

1. I. Teoh, M. Hung, J. Shieh, W.H. Lai, M.H. Hon, Electrochem. Solid-State Lett. **6**, G108 (2003)
2. E. Llobet, G. Molas, P. Molinàs, J. Calderer, X. Vilanova, J. Brezmes, J.E. Sueiras, X. Correig, J. Electrochem. Soc. **147**, 776 (2000)
3. J.L. Solis, A. Hoel, L.B. Kish, C.G. Granqvist, S. Saukko, V. Lantto, J. Am. Ceram. Soc. **84**, 1504 (2001)
4. M. Gillet, K. Aguir, M. Bendahan, P. Menneni, Thin Solid Films **484**, 358 (2005)
5. A. Michailowski, D. Aimawlawi, G. Cheng, M. Moskovits, Chem. Phys. Lett. **349**, 1 (2001)
6. Y. Huang, X.F. Duan, Q.Q. Wei, C.M. Lieber, Science **291**, 630 (2001)
7. H.J. Dai, Surf. Sci. **500**, 218 (2002)
8. Yong Shin Kim, Seung-Chul Ha, Kyuwon Kim, Haesik Yang, Sung-Yool Choi, Youn Tae Kim, Joon T. Park, Chang Hoon Lee, Jiyoung Choi, Jungsun Paek, Kwangyeol Lee, Appl. Phys. Lett. **86**, 213105 (2005)
9. Chao Li, Daihua Zhang, Xiaolei Liu, Song Han, Tao Tang, Jie Han, Chongwu Zhou, Appl. Phys. Lett. **82**, 1613 (2003)
10. M. Arnold, P. Avouris, Z.W. Pan, Z.L. Wang, J. Phys. Chem. B **107**, 659 (2003)
11. M. Law, H. Kind, B. Messer, F. Kim, P. Yang, Angew. Chem., Int. Ed. **41**, 2405 (2002)
12. A. Kolmakov, Y. Zhang, G. Cheng, M. Moskovits, Adv. Mater. **15**, 997 (2003)
13. C. Li, D. Zhang, X. Liu, S. Han, T. Tang, J. Han, C. Zhou, Appl. Phys. Lett. **82**, 1613 (2003)
14. Q. Wan, Q.H. Li, Y.J. Chen, T.H. Wang, X.L. He, J.P. Li, C.L. Li, Appl. Phys. Lett. **84**, 3654 (2004)
15. Gillet, R. Delamare, E. Gillet, J. Crys. Growth **279**, 93 (2005)
16. A. Magneli, Acta Chem. Scand. **7**, 315 (1953)
17. M. Gadenne, O. Schneegans, F. Houzé, P. Chrétien, C. Demarest, J. Sztern, P. Gadenne, Physica B **279**, 94 (2000)
18. M. Regragui, V. Jousseaume, M. Addou, B. El Idrissi, Thin Solid Films **397**, 238 (2001)